UV photodissociation of the van der Waals dimer $(CH_3I)_2$ revisited: Pathways giving rise to ionic features

Konstantin V. Vidma and Alexey V. Baklanov
Institute of Chemical Kinetics and Combustion, Institutskaja Street 3, Novosibirsk 630090, Russia

Evgeny B. Khvorostov, Valerii N. Ishchenko, and Sergei A. Kochubei
Institute of Semiconductor Physics, Academician Lavrentiev Ave. 13, Novosibirsk 630090, Russia

André T. J. B. Eppink
School of Chemistry, University of Leeds, Leeds LS2 9JT, United Kingdom

Dmitri A. Chestakov and David H. Parker[a)]
University of Nijmegen, Toernooiveld, Nijmegen 6525 ED, The Netherlands

(Received 22 March 2004; accepted 22 March 2005; published online 20 May 2005)

The CH_3I *A*-state-assisted photofragmentation of the $(CH_3I)_2$ van der Waals dimer at 248 nm and nearby wavelengths has been revisited experimentally using the time-of-flight mass spectrometry with supersonic and effusive molecular beams and the "velocity map imaging" technique. The processes underlying the appearance of two main $(CH_3I)_2$ cluster-specific features in the mass spectra, namely, I_2^+ and translationally "hot" I^+ ions, have been studied. Translationally hot I^+ ions with an average kinetic energy of 0.94 ± 0.02 eV appear in the one-quantum photodissociation of vibrationally excited $I_2^+(^2\Pi_{3/2,g})$ ions ($\langle E\rangle_{vib}=0.45\pm0.11$ eV) via a "parallel" photodissociation process with an anisotropy parameter $\beta=1.55\pm0.03$. Comparison of the images of I^+ arising from the photoexcitation of CH_3I clusters versus those from neutral I_2 shows that "concerted" photodissociation of the ionized $(CH_3I)_2^+$ dimer appears to be the most likely mechanism for the formation of molecular iodine ion I_2^+, instead of photoionization of neutral molecular iodine. © *2005 American Institute of Physics*. [DOI: 10.1063/1.1909083]

I. INTRODUCTION

Van der Waals (vdW) complexes are the first step of complexity along the way from isolated molecules to molecules in the condensed medium. The study of the photophysics and photochemistry of van der Waals complexes is vital in understanding the effect of a weakly bound environment on photoinitiated processes. In spite of the weak binding of partner molecules in the vdW complex, there are several examples in literature in which the vdW complex at low temperatures, or its analog (the "collisional complex") at higher temperatures, demonstrates "concerted" photochemistry, where new chemical channels open up as compared with the isolated molecule. Here we can refer to the iodine-containing dimers $(RI)_2$, giving rise to molecular iodine, which will be discussed in more detail below; dimers of OCS (Refs. 1 and 2) and CS_2,[3] generating S_2 as a photofragment; and the O_2-O_2 complex, giving rise to O_3+O;[4] as well as the O_2-N_2 complex, which gives two NO molecules as photoproducts.[5] The best documented example of this concerted photochemistry is the photodissociation of iodine-containing clusters $(RI)_n$, and the dimer $(RI)_2$ as the simplest member of this series. The photochemistry of van der Waals complexes $(RI)_n$ has been extensively studied during the last 15 years.[6–38] Special attention has been paid to $(CH_3I)_n$ (Refs. 6–31 and 36–38) and $(HI)_n$ (Refs. 20 and 31–35) clusters because of the large amount of data that is available concerning the photochemistry of the corresponding single molecules CH_3I and HI. Other kinds of *R* groups (such as CH_3CH_2, CF_3, etc.) have also been used[20] for cluster generation.

Various experimental approaches and detection techniques, such as time-of-flight mass spectrometry, laser-induced fluorescence (LIF), IR and UV absorption, and cavity ring-down spectroscopy (CRDS), have been used for the investigation of $(RI)_n$ clusters. Several groups have performed experiments involving photoexcitation of jet-cooled clustered CH_3I molecules in combination with ion time-of-flight detection of the photofragment mass spectrum.[6–18,38] Fan *et al.*[19–21] carried out LIF studies, and Wang *et al.*[22] performed resonance Raman scattering experiments. Donaldson *et al.*[23,24] carried out UV absorption studies of $(CH_3I)_n$ clusters, while Garvey and Bernstein[26] and Syage[27] reported on electron-impact investigations. One-quantum ionization of CH_3I clusters by vacuum ultraviolet (VUV) radiation was studied by Chen *et al.*[18] The IR-absorption spectra of matrix-isolated CH_3I clusters were obtained by Momose *et al.*[28] and Ito *et al.*[29] The photodissociation of $(HI)_n$ clusters was studied by Young[32,33] and by Zhang *et al.*[34] using the time-of-flight technique. Ito *et al.* have applied cavity ring-down spectroscopy (CRDS) in the region of the ν_1 band of CH_3I molecule to study $(CH_3I)_n$ cluster formation using super-

[a)]Author to whom correspondence should be addressed. Electronic mail: parker@sci.kun.nl

sonic jet conditions[39] and CRDS in visible has been applied for the study of I_2 product appearance in UV-photodissociation of $(CH_3I)_n$ clusters.[36]

Several groups have used the kinetic energy time-of-flight (KETOF)[12,13,32,33] analysis and ion imaging[37] to obtain information about the speed and angular distribution of the photofragments resulting from UV photoexcitation of $(CH_3I)_n$ (Refs. 12, 13, and 37) and $(HI)_n$.[32,33] Ito *et al.* performed *ab initio* calculations of the structure, binding energy, and vibrational wavenumbers of the dimer $(CH_3I)_2$ (Ref. 29) as well as the higher clusters $(CH_3I)_3$ and $(CH_3I)_4$.[39] Bogdanchikov *et al.*[40] carried out an *ab initio* study of the structure and binding energy of the isomers of the neutral dimer $(CH_3I)_2$ as well as its ionized form $(CH_3I)_2^+$.

The low temperature necessary to generate van der Waals complexes is provided by the technique of supersonic jet cooling. The efficiency of cooling and the cluster size depend on many parameters such as the backing pressure, the composition of the expanding mixture, etc. The formation of clusters as large as $(CH_3I)_8$ (Ref. 16) or even larger[10] has been detected. The effect of the backing pressure and the composition of the expanding mixture on the CH_3I cluster size distribution has been studied experimentally by Ito *et al.*[39]

As has been revealed in numerous previous studies, new photodissociation routes open up in clusters compared with the corresponding single molecules. The UV photodissociation of single CH_3I or HI molecules gives iodine atoms in the $^2P_{1/2}$ and $^2P_{3/2}$ states as well as CH_3 and H fragments, respectively.[41] Using conditions where the supersonic jet favors cluster formation, I_2^+ ions have been observed in the mass spectrum of the ionized species arising from the photoexcitation of CH_3I or HI clusters. Sapers *et al.*[6] observed the appearance of I_2^+ ions from clusters of CH_3I molecules when a nanosecond radiation of the KrF laser (248 nm) was used. Syage and Steadman[10] also reported the presence of I_2^+ in the mass spectrum of a cold beam of CH_3I molecules when a nanosecond or picosecond radiation at the wavelength of 266 nm was used. Strobel *et al.*[11] and Young[32,33] observed the appearance of the I_2^+ ion in the beams of CH_3I (Ref. 11) and HI (Refs. 32 and 33) molecules when excited at the 240-nm wavelength. Zhong *et al.*[14,15] and Poth *et al.*[16] observed a I_2^+ formation from CH_3I clusters in femtosecond pump-probe experiments using laser pulses at wavelengths of 277 plus 304 nm (Refs. 14 and 15) and 270 plus 405 nm.[16] Syage and Steadman studied these clusters with a picosecond pump-probe approach at wavelengths of 266 plus 532 nm.[10]

After the first observation of the I_2^+ formation by Sapers *et al.*,[6] efforts were made to analyze the mechanism of the $(CH_3I)_2$ photochemistry. The photoexcitation of $(CH_3I)_2$ yields I_2 (Refs. 19–22 and 36) and I_2^+,[6,10,14–16,31] which are new chemical channels compared to the monomer. In addition, energetic I^+ ions are observed.[37] Using UV photons around 250 nm, possible mechanisms for I_2, I_2^+, and I^+ formation include the following:

$$(CH_3I)_2 + h\nu \rightarrow I_2 + \text{other products}, \quad (1)$$

$$I_2 + 2h\nu \rightarrow I_2^+ + e^-, \quad (2)$$

$$I_2^+ + h\nu \rightarrow I^+ + I(^2P), \quad (3)$$

$$I_2 + h\nu \rightarrow I(^2P) + I(^2P), \quad (4)$$

$$I(^2P) + (2 \text{ or } 3)h\nu \rightarrow I^+ + e^-, \quad (5)$$

$$(CH_3I)_2 + 2h\nu \rightarrow (CH_3I)_2^+ + e^-, \quad (6)$$

$$(CH_3I)_2^+ + h\nu \rightarrow I_2^+ + \text{other products}. \quad (7)$$

Because I_2 formation [process (1)] has been observed in the experiments with CH_3I clusters, the I_2^+ and I^+ ions were usually assumed to appear due to the photodissociation and photoionization of I_2 [processes (2)–(5)]. However, these ions can be also formed via processes starting with the ionized dimer [process (7) followed by process (3)].

Some of the above-mentioned authors proposed that I_2^+ is the product of *dimer* photochemistry,[6,11,14,15,31] while others concluded that larger clusters also contribute to I_2^+ formation.[10,16,32,33] Poth *et al.*[16] suggested that the I_2^+ ion is produced via a dissociation of the ionic clusters $(CH_3I)_n^+$, as in process (6) for $n=2$. Syage and Steadman[10] studied the photodissociation of $(CH_3I)_n^+$ cluster ions at 532 nm [process (7)] and found that the photodissociation proceeds via the rupture of van der Waals bond and does not provide I_2^+ ions at this wavelength.

More information on the nature of the processes giving rise to ionic species in the photoexcitation of methyl iodide clusters can be gained from the energy distribution and angular anisotropy of the photofragments. In the current paper the ion time of flight and velocity map imaging techniques have been applied for the study of the cluster-specific pathways giving rise to ionic features under UV photoexcitation of methyl iodide dimer $(CH_3I)_2$.

II. EXPERIMENT

A. Time-of-flight experiments

For the present study two different experimental setups were used. The setup used in Novosibirsk is a molecular-beam apparatus combined with a time-of-flight mass spectrometer in the Wiley–McLaren arrangement.[42] The chamber is evacuated by a turbo-molecular pump and liquid N_2 trapping down to a pressure of 3×10^{-7} Torr. Two different molecular-beam arrangements were used with this setup. One arrangement provided a cold supersonic beam (estimated translational temperature of the gas in the probing region was as low as 1 K), and another one provided an effusive beam of gas at about room temperature. This allowed us to separately probe conditions favorable and unfavorable for the clustering of methyl iodide molecules. A home-built current-loop actuated valve similar to that one used in Ref. 43 generates the supersonic beam. The pulsed valve operates at 1 Hz with a pulse duration of 200 μs. Gas was expanded into the chamber through a 0.23-mm nozzle. The gas mixture was prepared by a flow of argon through a liquid CH_3I sample held at fixed temperatures provided by

different slush baths. This allowed us to vary the partial pressure of methyl iodide from 0.7 to 140 Torr. Mixtures of CH_3I (0.5%–1.5%) with a carrier gas (argon or helium) in a stainless steel vessel were also used. The valve backing pressure was varied within the interval of 0.2 to 2.5 bars. The gas jet passed through a 2.5-mm skimmer mounted 60 mm downstream and entered a homogeneous electric-field region created between the electrodes of the time-of-flight mass spectrometer (TOF MS), where it is crossed by a beam from a pulsed KrF excimer laser. Ions produced by laser radiation were accelerated by an electric field perpendicular to the directions of molecular and laser beams and detected by a microchannel plate (MCP) detector. The signal was then digitized, stored, and processed by a personal computer.

In the case of the effusive beam, the gas mixture flowed continuously into the chamber through a multichannel array (22×4 mm^2) with 50-μm channel diameter. The molecular beam was intersected 30 mm downstream by the laser beam. The nozzle was filled with neat CH_3I at pressures up to 0.25 Torr. The efficiency of cooling was negligible since the typical pore size was less than the gas-free path. Therefore, the molecules in the effusive beam were at room temperature.

Special attention was paid to create similar CH_3I concentration conditions in the supersonic and effusive molecular-beam setups. For the supersonic beam, the concentration of the carrier gas in the photoexcitation region was estimated by calculating the radial spread of the molecular beam using the formalism given in the paper of Anderson and Fenn.[44] In these estimations the effect of a small CH_3I admixture was neglected. The estimated concentrations of CH_3I molecules (the sum of clustered and unclustered species) in the excitation region were within the interval of $10^{11}-10^{13}$ cm^{-3} for the conditions used. The concentrations for the effusive beam were estimated with the use of the formalism for multichannel arrays given in the paper of Olander and Kruger.[45] These estimated concentrations for the effusive beam were within the interval of $2.5\times10^{11}-4.5\times10^{12}$ cm^{-3}.

A separate experiment on molecular iodine photoexcitation in the effusive beam conditions was also carried out. The molecular iodine vapor pressure of about 0.1 Torr was provided by a solid sample of I_2 connected to the volume behind the multichannel array. Its concentration in the photoexcitation region was estimated to be about 10^{12} cm^{-3}.

The home-built pulsed KrF excimer laser (248 nm) operated at 1 Hz with 1-mJ pulse energy and pulse duration of 5 ns. The light polarization was parallel ("vertical polarization") or perpendicular ("horizontal polarization") to the static electric field in the extracting region of the TOF MS where the photoexcitation took place. The laser beam was focused by a 53-cm focal length lens with a maximum laser-pulse energy fluence in the focal region of about 150 mJ/cm^2. The energy of the laser pulse was monitored by a UV-sensitive photodiode, which was mounted behind the output window of the chamber. Wire mesh or quartz filters were used to attenuate the pulse energy.

B. Velocity map imaging experiments

The Nijmegen velocity map imaging setup has been described in detail elsewhere.[46,47] The main feature of this setup is an electrostatic lens system using open electrodes for extracting nascent ions from the photoionization region through a time-of-flight region towards a two-dimensional (2D) spatial detector, which is gated at the proper arrival time for mass selection. The electrostatic lens is set to project all ions of the same velocity to the same point on the 2D detector, independent of their point of origin. The "velocity-mapped" 2D images contain all information about speed and angular distributions of photoproducts and can be reconstructed as three dimensional (3D) by applying the inverse Abel transform.

A brief overview of the experiment follows. The vacuum chamber was equipped with two pulsed solenoid valves (General Valves) providing the generation of the molecular beam directed parallel to the TOF axis (on-axis beam) or perpendicular to the TOF axis (off-axis beam). The results obtained with both configurations were similar; therefore only the experiments with the off-axis beam are described here. The molecular beam passed through a 2-mm skimmer mounted 20 mm downstream from the nozzle and propagates further perpendicular to the time-of-flight axis. About 100 mm downstream from the nozzle, the molecular beam enters the region between the repeller and extractor electrodes where photoexcitation takes place. In the experiments with methyl iodide the gas mixture contained 15–140 Torr of CH_3I and 1–2 bars of argon. Two modes of pulsed valve operation were used in order to change the conditions for cluster formation in the molecular beam. The conditions unfavorable for clustering were provided with a short gas pulse, while favorable clustering conditions were provided with a longer gas pulse. In the experiments with molecular iodine, the carrier gas flowed through a glass cylinder filled with iodine and was then injected in the chamber. The maximum partial pressure of molecular iodine in the injected gas mixture is estimated to be about 0.1–0.2 Torr. The lasers, valve, and detection equipment operated at a 10-Hz repetition rate.

The frequency-doubled radiation of a dye laser (Coumarin 500) pumped by the third harmonic of a neodymium-yttrium aluminum garnet (Nd-YAG) laser has been used for the generation of UV radiation tuned around 250 nm. The resulting pulse energy of this radiation was about 1 mJ and the pulse duration was about 5 ns. A lens with a focal length of 20 or 40 cm focused the light at the molecular beam. In experiments with clusters the laser power was adjusted to minimize the concentration of ions and to avoid their Coulomb repulsion by shifting the laser focus away from the molecular beam by 2–3 cm.

I^+ images were calibrated by the one-laser photodissociation of I_2 at different wavelengths used for (2+1) resonantly enhanced multiphoton ionization (REMPI) of $I(^2P_{3/2})$: at $\lambda_{vac}=249.61$ nm providing resonant two-quantum excitation to the intermediate level with an energy of $2h\nu=80125.45$ cm^{-1} (Ref. 48) or at $\lambda_{vac}=304.67$ nm.[47]

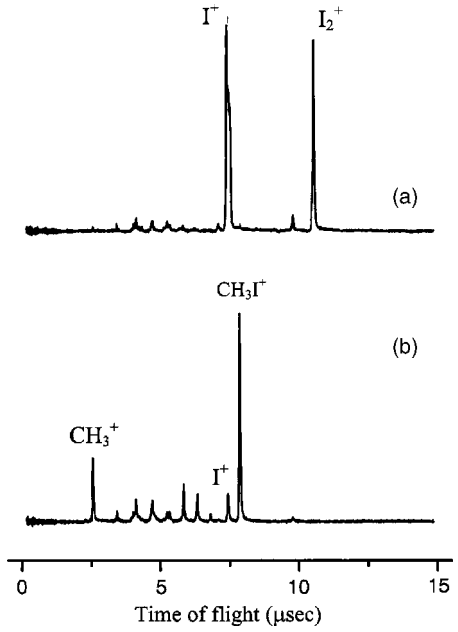

FIG. 1. Time-of-flight mass spectra of fragments resulting from the photodissociation of CH_3I molecules in (a) supersonic beam and (b) effusive beam, at the wavelength 248 nm. The unassigned peaks are due to the background.

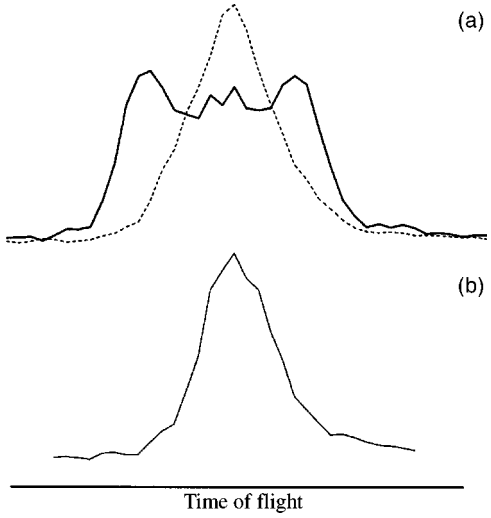

FIG. 2. Time-of-flight profiles of the I^+ peak arising from 248 nm photoexcitation of CH_3I molecules under the conditions of (a) supersonic beam and (b) effusive beam. Solid lines (—) correspond to the signal obtained with the laser radiation polarized parallel to the static electric field in the region of photoexcitation and the dotted line (···) corresponds to perpendicular polarization. The double peaking in signal observed for the supersonic beam (a) is due to hot I^+ ions with kinetic energy of about 1 eV. Monomer splitting [see also Fig. 6(a)] is too small to resolve under condition (b).

III. RESULTS

A. Mass spectra of CH_3I photodissociation fragments in effusive and supersonic beams

Time-of-flight mass spectra of ionized fragments of the photodissociation of CH_3I molecules at 248 nm (KrF laser) in supersonic and effusive beams are presented in Fig. 1. The laser power was the same for both spectra. The mass spectrum of the room-temperature effusive beam contains the parent ion CH_3I^+ as well as its photofragments I^+ and CH_3^+. In contrast, the mass spectrum with the supersonic beam shows the existence of strong I^+ and I_2^+ signal and the absence of CH_3I^+ and CH_3^+. Under clustering conditions a splitting of the I^+ peak [Fig. 2(a)] is seen, which disappears after changing the laser light polarization from parallel to perpendicular, relative to the static electric field. These features were also observed when helium, instead of argon, was used as a carrier gas. The mass spectrum did not change substantially when the laser pulse was scanned in time along the gas pulse. Data similar to those shown in Figs. 1 and 2 were observed for all concentrations of the precursor CH_3I molecules (estimated to be of $10^{11}-10^{13}$ cm^{-3} for the supersonic beam and $2.5\times10^{11}-4.5\times10^{12}$ cm^{-3} for the effusive beam).

A deconvolution of the time profile of the I^+ peak (Fig. 2) has been carried out. The form of the splitting is characteristic of a "parallel" photoprocess, and the peak separation corresponds to an I^+ ion kinetic energy of about 1 eV. Comparing the peak shape to one expected from a process with a purely parallel transition (anisotropy parameter $\beta=2$), it was determined that these "hot" ions provided about 70% of the total integral of the I^+ peak presented in Fig. 2(a). This contribution was dependent on the laser power, the backing pressure, and the CH_3I content in the molecular beam.

In Fig. 3, the laser-power dependence of the integrated I_2^+ and I^+ peaks as well as the sum of these peaks is shown. A drop in the I_2^+ signal due to the photodissociation is observed at higher pulse energy. This photodissociation gives rise to I^+ ions. The summed signal of I_2^+ and I^+ rises approximately with the square of the laser-pulse energy (the slope is equal to 2.36 ± 0.23). Taking into account that the hot component is the major component of the I^+ peak, we suppose that the hot I^+ ions arise primarily from the photodissociation of I_2^+.

To elucidate the size of the clusters that are the source of the cluster-specific features (I_2^+ and hot I^+) we have varied the expansion conditions in order to change the cluster size composition. The critical parameter for the cluster size composition is the CH_3I content in the expanding mixture. In Fig. 4 the experimentally measured ratio of the amplitudes of

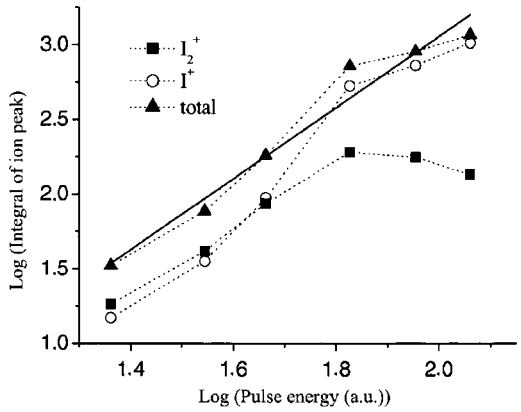

FIG. 3. The dependence of the integrals of I^+ and I_2^+ peaks on laser (248 nm) pulse energy in supersonic beam is shown. The symbol ■ corresponds to the I_2^+ peak; ○ corresponds to the I^+ peak; ▲ corresponds to the sum of the integrals of I^+ and I_2^+ peaks. Solid line indicates the linear fit for the ▲ dependence. The slope of fitted line is 2.36 ± 0.23. The expanded mixture was CH_3I (0.65%) in argon (2.5 bars).

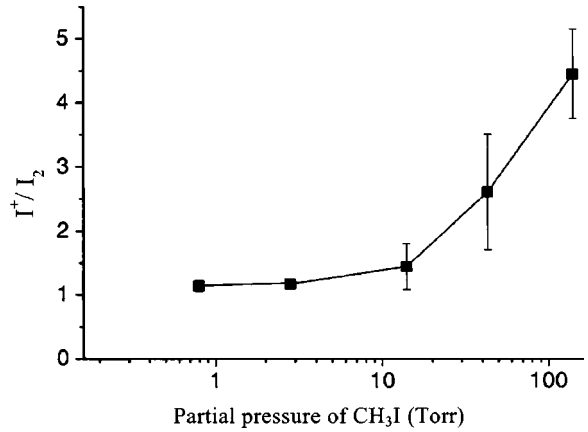

FIG. 4. The ratio of the amplitudes of the hot I^+ and I_2^+ peaks resulting from the photoexcitation of CH_3I clusters as a function of partial pressure of CH_3I in the expanding mixture. The stagnation pressure was 2.5 atm.

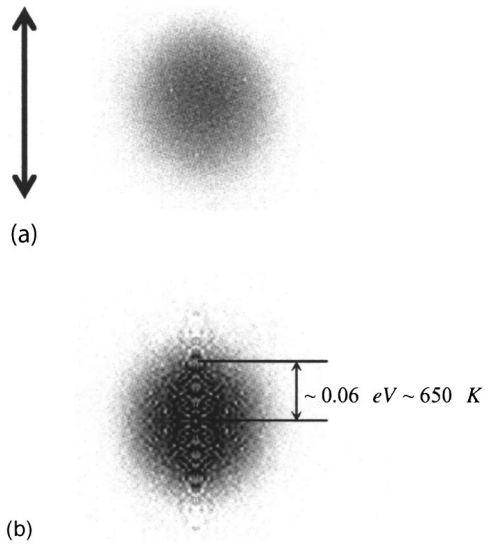

FIG. 5. Images of I_2^+ ions: (a) raw image and (b) reconstructed 3D velocity distribution. Laser polarization is shown by the double-headed arrow. The spacing of the lines in (b) indicate the velocity corresponding to the fitted translational temperature.

hot I^+ and I_2^+ signals due to cluster dissociation is shown as a function of the partial pressure of CH_3I (P_{CH3I}) in the expanding mixture. When P_{CH3I} decreased, the ratio stabilized to a constant value corresponding to the predominant dimers in the beam. The data from literature are in agreement with this conclusion. A substantial drop in the contribution of higher clusters with the decrease of the CH_3I partial pressure in the expanding mixture has been observed by Ito *et al.*[39] $(CH_3I)_n$ clusters of various size were detected in a series of papers where short-pulse lasers (picosecond or femtosecond)[10,14–17] as well as one-quantum VUV photoionization were used.[18] Syage and Steadman observed parent ions of clusters $(CH_3I)_n$ with $n \geqslant 8$ when the partial pressure of CH_3I was 60 Torr (carrier gas argon, backing pressure $P=1.6$ bar).[10] Poth *et al.*[16] observed clusters with n up to 8 with $P_{CH3I}=200$ Torr (carrier gas argon, backing pressure $P=3.3$ bars). Zhong and Zewail[15] used a lower pressure $P_{CH3I}=7-8$ Torr (carrier gas helium, backing pressure $P=1.3$ bar) and observed only the dimer $(CH_3I)_2$ without any traces of higher clusters. As it is shown in Fig. 4, we observed the cluster-specific features even for P_{CH3I} lower than 7–8 Torr. We can thus conclude that in the low CH_3I pressure extrapolation in our conditions (Fig. 4) the cluster features, I_2^+ and translationally hot I^+ in the TOF mass spectrum, are due to the photodissociation/photoionization of the $(CH_3I)_2$ dimers.

A separate experiment on the photoionization of pure molecular iodine at the wavelength of 248 nm was also performed to investigate the possibility that process (2), the two-photon ionization of the neutral I_2, provides the precursor of I_2^+ for our experimental conditions. Molecular iodine was introduced into the chamber under effusive beam conditions. The laser power and estimated concentration of I_2 molecules (10^{12} cm^{-3}) was similar to the concentration of CH_3I ($10^{11}-10^{13}$ cm^{-3}) in the supersonic beam experiment. The signals of I_2^+ and I^+ ions were negligible when using neat I_2 as a precursor.

B. Velocity map imaging

The velocity map imaging technique allowed us to obtain a detailed information on the speed and angular distributions of the I^+ and I_2^+ products of the $(CH_3I)_2$ photodissociation. The I_2^+ signal was observed only for conditions favorable for clustering in the molecular beam. A raw I_2^+ image is presented in Fig. 5(a) and its reconstructed 3D speed distribution is shown in Fig. 5(b). The reconstructed speed distribution was fit to a Maxwell distribution function, yielding a I_2^+ translational temperature of approximately 650 K. The angular distribution was found to be isotropic.

Figures 6(a) and 6(b) show I^+ images obtained under conditions favorable and unfavorable for cluster formation. The image corresponding to monomer dissociation [Fig. 6(a)] contains two main features: an outer ring and an inner structure. This image is very similar to the one reported by Samartzis *et al.*,[49] who studied the photodissociation of unclustered methyl iodide with a similar technique. They assigned the outer ring to the nonresonant two-photon ionization of $I(^2P_{1/2})$ atoms arising from the one-photon dissociation of CH_3I, and the lower-energy features arise from higher-order multiphoton processes. On tuning our laser to an $I^*(^2P_{1/2})$ resonance at 249.619 nm (vacuum) the outer ring is indeed greatly enhanced. Off-resonance, the I^+ image obtained for CH_3I monomers is much weaker than that obtained when clusters are present.

The I^+ image obtained at 248 nm under conditions favorable for cluster formation and low laser intensity (lens 2–3 cm out of focus) is shown in Fig. 6(b). Two main differences from the monomer image are: a smeared central "blob" instead of the sharp structure seen for the monomer and a large blurred outer ring of parallel character, which appears under the same molecular beam conditions as the I_2^+ signal. The origin of this outer ring will be discussed later in the text.

The radial speed distribution extracted from Fig. 6(b) is shown in Fig. 7(a). The two modes of this distribution were approximated by Gaussian functions. The best fit shows that the center of the outer ring distribution is located at

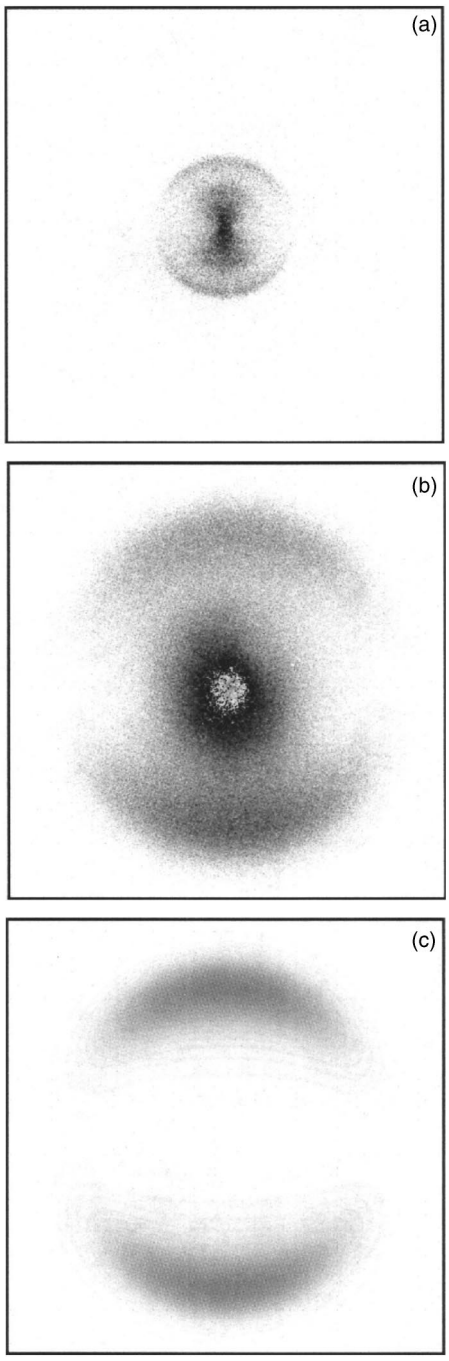

FIG. 6. (a) Raw image of I^+ obtained under nonclustering conditions. (b) Raw image of I^+ ions obtained under clustering conditions. Both images have the same scale. (c) Simulation of the outer ring of the experimental image as due to the process $I_2^+ + h\nu \rightarrow I + I^+$, where I_2^+ is formed with initial kinetic energy.

$E_t = 0.94 \pm 0.02$ eV, where the uncertainty is determined from averaging four experimental images. The angular distribution, Fig. 7(b), for this ring is fit by an anisotropy parameter of $\beta = 1.55 \pm 0.03$. The tuning of the UV-radiation wavelength over 1 nm to the blue and 6 nm to the red from 248.6 nm did not affect this hot-ion signal. The use of radiation resonantly enhancing the $I(^2P_{3/2})$ and $I(^2P_{1/2})$ signals (249.61 nm and 249.619 nm, respectively) did not affect the image of the hot I^+ ions. This result indicates that the neutral $I(I^*)$ atoms are not the precursors of the hot I^+ ions.

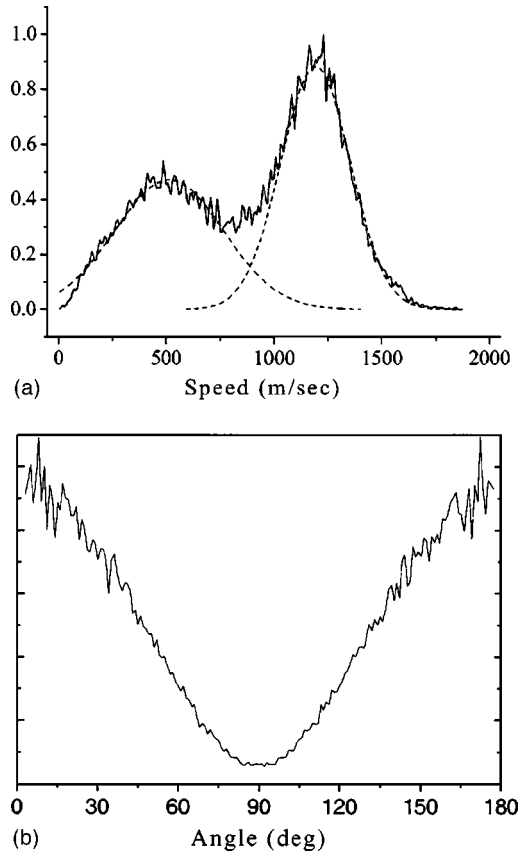

FIG. 7. (a) I^+ speed distribution from the image shown in Fig. 6(b). The center of the "outer ring" peak corresponds to an energy of 0.94 ± 0.02 eV. (b) Angular distribution of I^+ outer ring. The least squared fitting gives an anisotropy parameter value of $\beta = 1.55 \pm 0.03$.

C. Photodissociation of I_2 and I_2^+ around 248 nm

In order to identify the I_2^+ photodissociation channels giving rise to the observed hot I^+ ions, we have studied the photodissociation of I_2^+, which was generated via the two-photon ionization of the molecular iodine I_2. A one-laser setup was used with the laser wavelength $\lambda_{vac} = 248.6$ nm. It is known that I_2 shows only continuous absorption in this region. The two-quantum ionization of I_2 [process (2)] provides I_2^+, which absorbs an extra photon and gives rise to an I^+ ion. In all the experiments with molecular iodine, I^+ images were observed only when the laser focus was set at the molecular beam. The image of I^+ appearing in the process $I_2^+ + h\nu \rightarrow I^+ + I(I^*)$ is presented in Fig. 8(a). The reconstructed total kinetic energy release (TKER) distribution is shown in Fig. 8(b).

At the wavelength $\lambda_{vac} = 248.6$ nm ($h\nu = 4.99$ eV), a two-quantum photoionization can produce molecular ion I_2^+ in its two lowest spin–orbit $^2\Pi_{3/2,g}$ and $^2\Pi_{1/2,g}$ substates, with an adiabatic ionization energy determined by Cockett *et al.*[50] to be 9.31 and 9.95 eV, respectively. When the photon energy was tuned below the threshold for the two-quantum ionization into the $^2\Pi_{1/2,g}$ state of the I_2^+ ($\lambda_{vac} > 249.2$ nm), peak 1 from Fig. 8 changed slightly in energy but peaks 2 and 3 with the TKER centered at 2.08 and 3.02 eV disappeared. This allowed us to identify peaks 2 and 3 as belonging to channels of the $I_2^+(^2\Pi_{1/2,g})$ photodissociation. The anisotropy parameter for channel 1 was found to be $\beta = 1.58 \pm 0.03$. Fig-

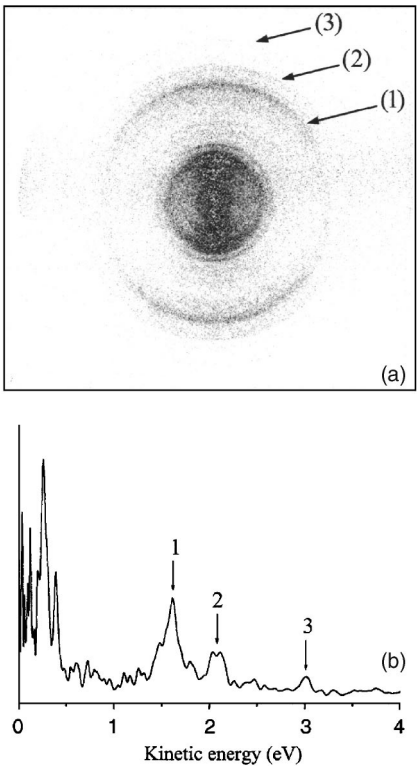

FIG. 8. (a) Raw image of I^+ ions resulting from the photoexcitation of I_2 at the wavelength 248.6 nm. (b) Reconstructed total kinetic energy distribution (TKER) for the process $I_2^+ + h\nu \rightarrow I + I^+$. Channel (1) corresponds to 1.61-eV TKER at maximum, channel (2) corresponds to 2.08-eV TKER, and channel (3) corresponds to 3.02-eV TKER. Several unassigned rings in the central part of the image correspond to the TKER below 0.4 eV.

ure 9 shows an energy diagram for the $I_2^+(v=0)$ photodissociation at 248 nm. Peaks 2 and 3 from Fig. 8 coincide well with the TKER expected for I^+ ions produced from low v-state vibrationally excited $I_2^+(^2\Pi_{1/2,g})$ dissociated to the $[I^+(^3P_{1,0}) + I(^2P_{3/2})]$ and $[I^+(^3P_2) + I(^2P_{3/2})]$ products, respectively, while peak 1 corresponds to production starting from $I_2^+(^2\Pi_{3/2,g})$ dissociated to $[I^+(^3P_{1,0}) + I(^2P_{3/2})]$.

To check the possibility that I_2 is a precursor of the I^+ observed in the experiments with clusters of CH_3I, we tuned the laser to the wavelength $\lambda_{vac} = 249.61$ nm, which is in resonance with a two-photon transition from the ground-state $I(^2P_{3/2})$ to the $(^1D_2)\ 6p[2]_{2\ 1/2}$ state ($E = 80\,125.45\ cm^{-1}$).[48] Figure 10 shows images of I^+ due to (2+1) REMPI of $I(^2P_{3/2})$ [Fig. 10(a)] arising from the photodissociation of molecular iodine,

$$I_2(X^1\Sigma_g) \xrightarrow{h\nu} I(^2P_{3/2}) + I(^2P_{1/2}), \quad \Delta E = -1.50\ \text{eV}, \tag{4'}$$

and from the photoexcitation of CH_3I clusters [Fig. 10(b)]. The anisotropy parameter of process (4′) was found to be $\beta = -0.89 \pm 0.01$. A comparison of the two images in Fig. 10 shows that the I^+ outer ring from the $(CH_3I)_2$ dimer does not come from the neutral I_2 molecules. The strong signal at lower kinetic energy in this image [Fig. 10(b)] results from the resonant detection of $I(^2P_{3/2})$ atoms arising from the dissociation of CH_3I monomers in the beam.

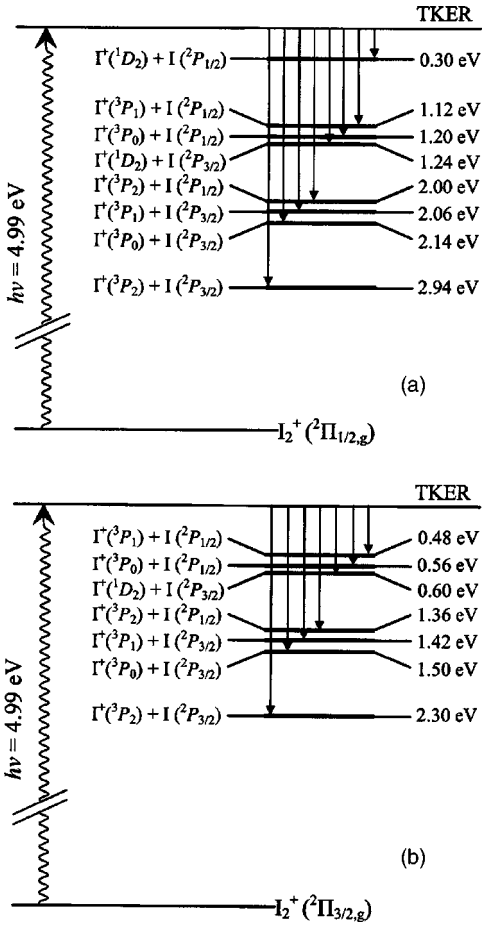

FIG. 9. The energy scheme of possible channels of (a) $I_2^+(^2\Pi_{1/2})$ and (b) $I_2^+(^2\Pi_{3/2})$ photodissociation at $\lambda_{vac} = 248.6$ nm. The energies of the states of I_2^+ ion were taken from the paper by Cockett *et al.* (Ref. 50). The energies of I and I^+ states were taken from the tables by Moore (Ref. 51). In the calculation, the ions $I_2^+(^2\Pi_{1/2,g})$ and $I_2^+(^2\Pi_{3/2,g})$ were assumed to be vibrationally unexcited.

IV. DISCUSSION

A. Translationally hot I^+ ions

The translationally hot I^+ ions shown in Figs. 6 and 10 arise from a precursor with a rather broad absorption spectrum, which could be I_2^+. They cannot be a result of resonant ionization of fast neutral I atoms because the signal of hot I^+ ions was not effected by tuning the laser to the resonant transitions of $I(I^*)$ atoms. As seen from Fig. 3, the photodissociation of I_2^+ takes place at higher laser-pulse energy values and is accompanied by a rise in the I^+ signal. As we have found above, about 70% of the I^+ signal in the TOF experiments is contributed by hot I^+ ions. In the imaging experiments, the hot I^+ ions appear only together with an I_2^+ signal. Another argument comes from the shape of the image of these hot I^+ ions [outer ring on Fig. 6(b)] which is rather blurry. The most probable reason for the image broadening is the effect of velocity distribution of the precursor. The translational temperature of 650 K of I_2^+ extracted from the image in Fig. 5 was then used for the simulation of the image of I^+ arising from this precursor. The result of the simulation is shown in Fig. 6(c) and is very similar to the image observed experimentally for hot I^+ ions [outer ring in Fig. 6(b)]. We

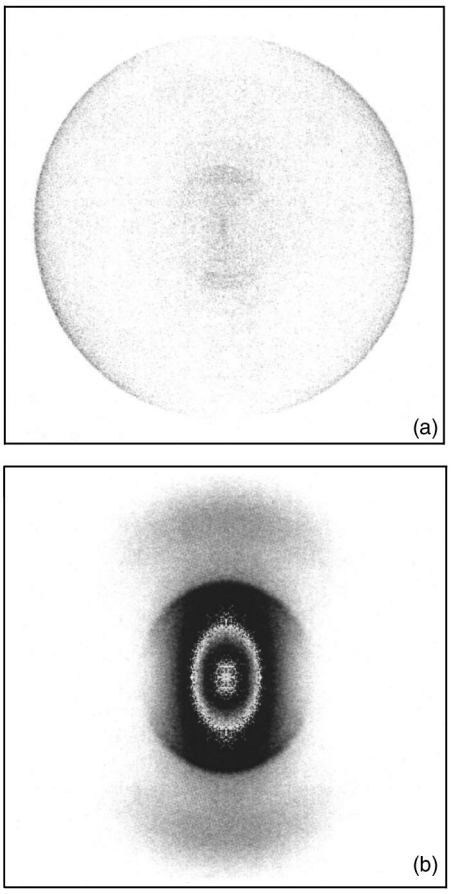

FIG. 10. (a) I^+ image taken with $I(^2P_{3/2})$ (2+1) REMPI at 249.61 nm and a sample of neat I_2. The outer ring corresponds to the one-photon dissociation of neutral I_2 [process (4′)] in the text. (b) Image of I^+ ions resulting from $(CH_3I)_2$ dimer photoexcitation at 249.61 nm.

can thus conclude that I_2^+ is a precursor of the hot I^+ ions with an average translational energy of $E_t=0.94\pm0.02$ eV. In the photodissociation process (3) $I_2^+ + h\nu \rightarrow I^+ + I(I^*)$, two fragments of equal mass appear. The total kinetic energy release (TKER) in this process is equal to double the value of E_t, i.e., TKER $=1.88\pm0.04$ eV.

In order to establish the channel giving rise to these hot I^+ ions we consider the experimental results of the photodissociation of I_2^+ generated via the two-quantum photoionization of the neutral I_2 (Fig. 8) and the possible channels of I_2^+ photodissociation (Fig. 9). The region of the TKER values below 0.5 eV (Fig. 8) involves the channels corresponding to the I_2^+ photodissociation as well as the channels due to the photodissociation/photoionization of the CH_3I residue, which was also observed as a background in the experiments with I_2. At higher TKER [Fig. 8(b)], peaks 1 and 2 centered at 1.61 and 2.08 eV are closest to the experimentally determined TKER $=1.88\pm0.04$ eV value. Peak 2 (Fig. 8) can be due to several overlapping peaks, which is possible, considering the energy level structure shown in Fig. 9. In this case, peak 2 corresponds to the photodissociation of the excited state $I_2^+(^2\Pi_{1/2,g})$ and has a TKER higher than 1.88 eV.

Peak 1 (Fig. 8) at 1.61 eV appears to be responsible for the hot I^+ peak observed in the cluster experiment. This peak is the brightest of the high TKER peaks. Its anisotropy parameter $\beta=1.58\pm0.03$ measured in I_2^+ photodissociation coincides well with the parameter $\beta=1.55\pm0.03$ measured for hot I^+ in the CH_3I cluster experiments. This peak corresponds to the photodissociation of ground-state $I_2^+(^2\Pi_{3/2,g})$ ions via one or several closely lying channels, which, for vibrationally unexcited ions, yield a TKER value of 1.43 ± 0.07 eV. For the experiments with I_2, the 1.61-eV TKER measured for this channel can be explained by the vibrational excitation of I_2^+ ions, caused by the difference in equilibrium geometry of the neutral $I_2(r_e(I-I)=2.666$ Å$)$[52] and the ionic $I_2^+(r_e(I-I)=2.57$ Å$)$.[53] For the experiments with $(CH_3I)_2$, the TKER value of 1.88 ± 0.04 eV measured for this channel indicates that $I_2^+(^2\Pi_{3/2,g})$ ions appear with a vibrational excitation of 0.45 ± 0.11 eV and that very few $I_2^+(^2\Pi_{1/2,g})$ ions are formed.

As we mentioned above, a possible model for the I_2^+ formation from $(CH_3I)_2$ involves process (2), the photoionization of neutral molecular iodine. Using the data of Fig. 10, we demonstrate that neutral molecular iodine I_2 is not a precursor of the I_2^+ appearing after the photoexcitation of the $(CH_3I)_2$ dimer. Figure 10(a) shows that (2+1) REMPI $I(^2P_{3/2})$ atom signal from I_2 photodissociation yields a "perpendicular" I^+ image. The perpendicular character ($\beta=-0.89$) is in agreement with the earlier result of Clear and Wilson,[54] who studied the photodissociation of I_2 at the nearby lying wavelength of 266 nm and found $\beta\sim-1$. Under the conditions of our experiment, the two-quantum photoionization of I_2 also takes place, as well as the subsequent photodissociation of the resulting I_2^+, giving rise to I^+. In Fig. 10(a) there is also a parallel ring of I^+ due to the photodissociation of I_2^+ (the same as ring and peak 1 in Fig. 8), but it is dramatically less intense than the simultaneously observed signal due to the REMPI of the neutral $I(^2P_{3/2})$. The I^+ image of Fig. 10(b) shows that in the case of the CH_3I cluster experiment at the same wavelength, we observe the opposite situation: that is, the parallel image due to hot I^+ ions is intense when the perpendicular image due to the REMPI of the neutral $I(^2P_{3/2})$ is absent. This means that the contribution of the neutral I_2 as a precursor of I_2^+ in the dimer $(CH_3I)_2$ photoexcitation is negligible.

In principle, the measurements analogous to those shown in Fig. 10, when carried out under similar laser power conditions for neat I_2 and for CH_3I clusters, could allow us to estimate the yield of molecular I_2 via process (1), which was observed earlier experimentally.[19–22,36] We should mention again that in our experiment with neutral I_2 [Fig. 10(a)] the laser radiation was tightly focused, but that in the experiment with clusters [Fig. 10(b)] we had to lower the laser intensity by shifting the laser focus away from the molecular beam in order to obtain an image that was not distorted by Coulomb repulsion of the abundantly formed ions from CH_3I and CH_3I^+ ionization/dissociation [central part in Fig. 10(b)]. This did not allow us to use the same laser power conditions in these experiments, and thus we could not estimate the yield of I_2 via process (1).

B. Dissociation of the ionized $(CH_3I)_2^+$ dimer

An alternative source of I_2^+ is the dissociation of the ionized $(CH_3I)_2^+$ dimer, process (7). There is no reason to expect

a reduction of the photoionization yield in the dimer as compared with the free CH_3I molecule. The results of our experiments with supersonic and effusive beams show that the total yield of ions under clustering conditions is higher than for the unclustered case. At a VUV photon energy close to two quanta of the KrF laser ($\approx$10 eV), Chen *et al.*[18] observed a parent ion $(CH_3I)_2^+$ as the main product among the ions appearing from the photoionization of the neutral $(CH_3I)_2$ dimer. However, we do not observe any $(CH_3I)_2^+$ ions in the case of dimer photoionization. We suspect that the photoionization of the dimer is followed by a spontaneous or photoinitiated decay of the ionized dimer, giving rise to I_2^+. The energy of two UV quanta of the KrF laser ($2h\nu$=9.97 eV) is higher than the energy of the fragments of the spontaneous decay of $(CH_3I)_2^+$ via

$$(CH_3I)_2 + 2h\nu \rightarrow [(CH_3I)_2^+]^* \rightarrow I_2^+ + C_2H_6, \quad \Delta E = -1.09 \text{ eV}. \tag{8}$$

The calculated ΔE value has been obtained with the use of the enthalpy data for CH_3I, C_2H_6 and I_2 molecules[55] and the ionization potential (IP) of I_2[50] as well as the *ab initio* calculated binding energy (0.096 eV) in the $(CH_3I)_2$ van der Waals dimer.[40] In spite of the exothermicity of process (8), the formation of I_2^+ was not observed by Chen *et al.*,[8] who studied the photoionization of CH_3I clusters in a one-quantum process with the quantum energy tuned within the range of 8–35 eV. This result of Chen *et al.* does not exclude process (8) in our case because a two-quantum ionization of $(CH_3I)_2$ can yield $(CH_3I)_2^+$ ions with higher vibrational excitation, and thus a different decay rate than one-quantum ionization. The absence of $(CH_3I)_2^+$ and presence of I_2^+ can be also due to the photodissociation of $(CH_3I)_2^+$ ions by a photon of the same laser pulse

$$(CH_3I)_2^+ \xrightarrow{h\nu} I_2^+(^2\Pi_{3/2,g}) + 2CH_3, \quad \Delta E = -2.27 \text{ eV}, \tag{7'}$$

$$\xrightarrow{h\nu} I_2^+(^2\Pi_{3/2,g}) + C_2H_6, \quad \Delta E = -6.08 \text{ eV}. \tag{7''}$$

The enthalpy value for CH_3 is taken from Ref. 55. An absorption cross section at 248.6 nm higher than 3×10^{-17} cm^2 will result in photodissociation of more than 99% of the $(CH_3I)_2^+$ precursor ions. This value of the cross section implies saturation of the third photon absorption step and a near-quadratic pulse-energy dependence of the I_2^+ yield, as found in our experiments (the total yield of I_2^+ and I^+ arising from I_2^+ increased at a power of 2.36 ± 0.23 pulse energy).

C. Discussion of the previous data on hot I^+ ions

The previous results of Tanaka *et al.*[37] can be interpreted using the same line of reasoning as above. Tanaka *et al.* used ion imaging for the study of the photofragments of CH_3I cluster photodissociation at 266 nm and observed the formation of hot I^+ ions with translational energy E_t=0.69 and 1.08 eV appearing via parallel processes with $\beta = 2 \pm 0.6$ and 2 ± 0.5, correspondingly. The authors[37] suggested that these hot ions are due to fast I atoms arising from the photodissociation of the CH_3I moiety in small clusters. Taking into account our results, we can interpret these hot ions as due to the one-quantum photodissociation of $I_2^+(^2\Pi_{3/2,g})$ via the lowest channels shown in Fig. 9(b). The difference of 0.39 eV (an experimental uncertainty is not given in Ref. 37) in the values of E_t for the channels observed by Tanaka *et al.* corresponds to a difference of 0.78 eV in the TKER values, which is very close to the energy gap of 0.8 eV for these channels [Fig. 9(b)]. The channel with E_t=0.69 eV (TKER =1.38 eV) in the experiments of Tanaka *et al.* is similar to the channel we observed (TKER=1.88 ± 0.04 eV). The difference in the TKER values is partially due to the difference in the quantum energy ($h\nu$=4.66 eV at 266 nm versus $h\nu$ =4.99 eV at 248.6 nm). An extra 0.17 eV in the TKER difference can be due to a variation in the vibrational excitation of I_2^+ with the dissociation wavelength. We should also mention that at 248.6 nm the lowest channel of Fig. 9(b) was also observed in the case of I_2^+ dissociation (a weak parallel ring with E_t about 2.4 eV between rings 2 and 3 in Fig. 8). This gave a rather low contribution and was not distinct in our experiments with clusters (Fig. 6). Probably, the ratio of the product channels of I_2^+ photodissociation is wavelength dependent. The formation of hot I^+ ions with E_t=0.924 eV and a high anisotropy ($\beta \geqslant 1.5$) was also observed by Young, who studied the photodissociation of the clusters $(HI)_n$ at 240 nm.[32] The similarity of E_t and anisotropy with our observations suggests that the $I_2^+(^2\Pi_{3/2,g})$ ion is a precursor of hot I^+ ions in the cited experiments of Young as well.

D. Previous experiments concerning the dissociation of the ionized $(CH_3I)_2^+$ dimer

Syage and Steadman[10] studied the 532-nm photodissociation of $(CH_3I)_2^+$ dimer ions prepared from the neutral dimer by electron impact. They observed the photodissociation of the ionized dimer only via the van der Waals bond $(CH_3I)_2^+ + h\nu \rightarrow CH_3I^+ + CH_3I$ and concluded that the photoexcitation of dimer ions does not contribute substantially to the production of ionized fragments such as I_2^+. Because the result of Syage and Steadman was obtained at 532 nm, far from the UV region, it does not contradict our conclusion that the ionized dimer is the source of I_2^+ in the UV photochemistry of CH_3I clusters.

The difference in energy of the products of process (7′) and the neutral dimer $(CH_3I)_2$ is 12.69 eV. The process of dissociative ionization of the dimer,

$$[(CH_3I)_2]^* \rightarrow CH_3I^+ + CH_3I \ \Delta E_{\text{thresh}} = 9.64 \text{ eV}, \tag{9}$$

has a ΔE_{thresh} value calculated on the basis of IP (CH_3I) =9.54 eV (Ref. 56) and a binding energy of 0.096 eV for the vdW dimer $(CH_3I)_2$.[40] The $(CH_3I)_2^+$ ions prepared by electron impact[10] that survived until the arrival of the dissociation laser pulse should have an internal energy close to or lower than ΔE_{thresh}. The sum of ΔE_{thresh}=9.64 eV and energy of the quantum of radiation at 532 nm $h\nu$=2.33 eV gives the value 11.97 eV, which is less than the 12.69 eV required for channel (7′) to be observed.

Channel (7″) lies 0.7 eV lower than the dissociative ionization of the dimer into $CH_3I^+ + CH_3I$ [channel (9)]. But channel (7″) is a four-centered reaction which should have a

large activation barrier according to the Woodward–Hoffman correlation rules. For this reason channel (7″) could probably not compete with the dissociative ionization [process (9)] in the experiments of Syage and Steadman, if the dissociation of ionized dimer was "statistical" as supposed by the authors. Due to the same reason we are in doubt about spontaneous decay [channel (8)] as the source for I_2^+ formation.

Channel (7′) lies higher in energy than the dissociative ionization [channel (9)] and probably higher than the activation barriers for channel (7″). This channel can become accessible when using UV photoexcitation. The photodissociation of $(CH_3I)_2^+$ ions in the UV region could be nonstatistical, particularly if the excited state is repulsive. We suggest that the source of I_2^+ ions observed in the UV photochemistry of CH_3I dimers involves photodissociation of the ionized dimer $(CH_3I)_2^+$ via channel (7′). In our previous paper *ab initio* calculations have been carried out on the energetics and geometry of the neutral and ionized dimers of CH_3I.[40] These calculations have shown that the strong binding between the ionized pair of I atoms exists in the most stable head-to-head configuration of the ion $(CH_3I)_2^+$. In this ion the spin density is already uniformly distributed over two I atoms and the distance $r_e(I–I)=3.14$ Å is quite close to the distance in the ion I_2^+ (2.57 Å).[53] The structure of the $(CH_3I)_2^+$ ion thus favors the formation of I_2^+ as a product.

V. CONCLUSIONS

The CH_3I *A*-state-assisted photofragmentation of the van der Waals dimer $(CH_3I)_2$ has been investigated with the use of the time-of-flight and "velocity map imaging" techniques for excitation around 248 nm. The main features in the mass spectrum of the dimer $(CH_3I)_2$ photofragments as compared with the photodissociation of single CH_3I molecules were observed: molecular ions I_2^+ (translational temperature, 650 K) and translationally hot I^+ ions ($E_t=0.94\pm0.02$ eV, anisotropy parameter $\beta=1.55\pm0.03$). It was found that hot I^+ ions arise from the photodissociation of I_2^+ ions in their electronic ground state ($^2\Pi_{3/2,g}$), and the vibrational energy of the nascent I_2^+ ions was determined to be 0.45 ± 0.11 eV. A comparison of the images of I^+ arising in the photoexcitation of CH_3I clusters with the neutral I_2 has allowed us to neglect the molecular iodine as the precursor of I_2^+ in the mass spectrum of the photofragments. The concerted photodissociation of the ionized dimer $(CH_3I)_2^+$ was concluded to be the most probable source of the molecular iodine ion I_2^+.

ACKNOWLEDGMENTS

The financial support of this work by the Netherlands Organization for Scientific Research (NWO) under the programs NWO (FOM-MAP) and NWO Russia-Netherlands Cooperative Research Grant No. 047.009.001, the Russian Foundation for Basic Research (Grant No. N 02-03-32001), and the Russian Ministry of Education (Grant No. N E02-3.2-51) is gratefully acknowledged. A.T.J.B.E. is grateful to the European Union for a postdoctoral fellowship funded through the PICNIC HPRN-CT-2002-00183 network.

[1] N. J. A. van Veen, P. Brewer, P. Das, and R. Bersohn, J. Chem. Phys. **79**, 4295 (1983).
[2] N. Sivakumar, I. Burak, W.-Y. Cheung, P. L. Houston, and J. W. Hepburn, J. Phys. Chem. **89**, 3609 (1985).
[3] W.-B. Tzeng, H.-M. Yin, W. Y. Leung, J. Y. Luo, S. Nourbakhsh, G. D. Flesh, and C. Y. Ng, J. Chem. Phys. **88**, 1658 (1988).
[4] L. Brown and V. Vaida, J. Phys. Chem. **100**, 7849 (1996).
[5] E. C. Zipf and S. S. Prasad, J. Chem. Phys. **115**, 5703 (2001).
[6] S. P. Sapers, V. Vaida, and R. Naaman, J. Chem. Phys. **88**, 3638 (1988).
[7] R. O. Loo, H. P. Haerri, G. E. Hall, and P. L. Houston, J. Phys. Chem. **92**, 5 (1988).
[8] S. M. Penn, C. C. Hayden, K. J. Carlson Muyskens, and F. F. Crim, J. Chem. Phys. **89**, 2909 (1988).
[9] R. O. Loo, H. P. Haerri, G. E. Hall, and P. L. Houston, J. Chem. Phys. **90**, 4222 (1989).
[10] J. A. Syage and J. Steadman, Chem. Phys. Lett. **166**, 159 (1990).
[11] A. Strobel, I. Fischer, A. Lochschmidt, K. Muller-Dethlefs, and V. E. Bondybey, J. Phys. Chem. **98**, 2024 (1994).
[12] J. A. Syage, Chem. Phys. Lett. **245**, 605 (1995).
[13] J. A. Syage, Chem. Phys. **207**, 411 (1996).
[14] D. Zhong, P. Y. Cheng, and A. H. Zewail, J. Chem. Phys. **105**, 7864 (1996).
[15] D. Zhong and A. H. Zewail, J. Phys. Chem. A **102**, 4031 (1998).
[16] L. Poth, Q. Zhong, J. V. Ford, and A. W. Castleman, Jr., J. Chem. Phys. **109**, 4791 (1998).
[17] J. V. Ford, Q. Zhong, L. Poth, and A. W. Castleman, J. Chem. Phys. **110**, 6257 (1999).
[18] J. Chen, L. Pei, J. Shu, C. Chen, X. Ma, L. Shen, and Y. W. Zhang, Chem. Phys. Lett. **345**, 57 (2001).
[19] Y. B. Fan and D. J. Donaldson, J. Phys. Chem. **96**, 19 (1992).
[20] Y. B. Fan, K. L. Randall, and D. J. Donaldson, J. Chem. Phys. **98**, 4700 (1993).
[21] Y. B. Fan and D. J. Donaldson, J. Chem. Phys. **97**, 189 (1992).
[22] P. G. Wang, Y. B. Zhang, C. J. Ruggles, and L. D. Zeigler, J. Chem. Phys. **92**, 2806 (1990).
[23] D. J. Donaldson, V. Vaida, and R. Naaman, J. Chem. Phys. **87**, 2522 (1987).
[24] D. J. Donaldson, V. Vaida, and R. Naaman, J. Phys. Chem. **92**, 1204 (1988).
[25] G. C. G. Washewsky, R. Horansky, and V. Vaida, J. Phys. Chem. **100**, 11559 (1996).
[26] J. F. Garvey and R. B. Bernstein, J. Phys. Chem. **90**, 3577 (1986).
[27] J. A. Syage, J. Chem. Phys. **92**, 1804 (1990).
[28] T. Momose, M. Miki, M. Uchida, T. Shimizu, I. Yoshizawa, and T. Shida, J. Chem. Phys. **103**, 1400 (1995).
[29] F. Ito, T. Nakanaga, Y. Futami, S. Kidoh, M. Takayanagi, and M. Nakata, Chem. Phys. Lett. **343**, 185 (2001).
[30] H. Korneweitz and R. D. Levine, Chem. Phys. Lett. **294**, 153 (1998).
[31] V. Vaida, D. J. Donaldson, S. P. Sapers, R. Naaman, and M. S. Child, J. Phys. Chem. **93**, 513 (1989).
[32] M. A. Young, J. Chem. Phys. **102**, 7925 (1995).
[33] M. A. Young, J. Phys. Chem. **98**, 7790 (1994).
[34] J. Zhang, M. Dulligan, J. Segall, Y. Wen, and C. Witting, J. Phys. Chem. **99**, 13680 (1995).
[35] K. L. Randall and D. J. Donaldson, J. Chem. Phys. **18**, 6763 (1995).
[36] F. Ito and T. Nakanaga, J. Chem. Phys. **119**, 5527 (2003).
[37] Y. Tanaka, M. Kawasaki, and Y. Matsumi, Bull. Chem. Soc. Jpn. **71**, 2539 (1998).
[38] Y. K. Choi, Y. M. Koo, and K. W. Jung, J. Photochem. Photobiol., A **127**, 1 (1999).
[39] F. Ito, T. Nakanaga, Y. Futami, and M. Nakata, Chem. Phys. **286**, 337 (2003).
[40] G. A. Bogdanchikov, A. V. Baklanov, and D. H. Parker, Chem. Phys. Lett. **376**, 395 (2003).
[41] H. Okabe, *Photochemistry of Small Molecules* (Wiley-Interscience, New York, 1978).
[42] W. C. Wiley and I. H. McLaren, Rev. Sci. Instrum. **26**, 1150 (1955).
[43] V. I. Ishchenko, S. A. Kochubei, V. I. Makarov, and I. V. Khmelinskii, Chem. Phys. Lett. **299**, 227 (1999).
[44] J. B. Anderson and J. B. Fenn, Phys. Fluids **8**, 780 (1965).
[45] D. R. Olander and V. Kruger, J. Appl. Phys. **41**, 2769 (1970).
[46] A. T. J. B. Eppink and D. H. Parker, Rev. Sci. Instrum. **68**, 3477 (1997).
[47] A. T. J. B. Eppink and D. H. Parker, J. Chem. Phys. **109**, 4758 (1998).
[48] L. Minnhagen, Ark. Fys. **21**, 415 (1962).

[49]P. C. Samartzis, B. L. G. Bakker, D. H. Parker, and T. N. Kitsopoulos, J. Phys. Chem. A **103**, 6106 (1999).
[50]M. C. R. Cockett, J. G. Goode, K. P. Lawley, and R. J. Donovan, J. Chem. Phys. **102**, 5226 (1995).
[51]C. E. Moore, NBS Circular No. 476, 1958.
[52]K. P. Huber and G. Herzberg, Constants of Diatomic Molecules, in NIST Chemistry WebBook, edited by P. J. Linstrom and W. G. Mallard (http://webbook.nist.gov).
[53]S. M. Mason and R. P. Tuckett, Chem. Phys. Lett. **160**, 575 (1989).
[54]R. D. Clear and K. R. Wilson, J. Mol. Spectrosc. **47**, 39 (1973).
[55]*Thermodynamical Properties of the Individual Substances* (in Russian), 3rd ed., edited by V. P. Glushko (Nauka, Moscow, 1978).
[56]*CRC Handbook of Chemistry and Physics*, 77th ed., edited by D. R. Lide (CRC: Boca Raton, FL, 1997).